

# Analysis of the electrical properties of Cr/n-BaSi<sub>2</sub> Schottky junction and n-BaSi<sub>2</sub>/p-Si heterojunction diodes for solar cell applications

著者別名	都甲 薫, 末益 崇
journal or publication title	Journal of applied physics
volume	115
number	22
page range	223701
year	2014-06
権利	(C) 2014 AIP Publishing LLC This article may be downloaded for personal use only. Any other use requires prior permission of the author and the American Institute of Physics. The following article appeared in J. Appl. Phys. 115, 223701 (2014) and may be found at <a href="http://dx.doi.org/10.1063/1.4882117">http://dx.doi.org/10.1063/1.4882117</a> .
URL	<a href="http://hdl.handle.net/2241/00121623">http://hdl.handle.net/2241/00121623</a>

doi: 10.1063/1.4882117

## Analysis of the electrical properties of Cr/n-BaSi<sub>2</sub> Schottky junction and n-BaSi<sub>2</sub>/p-Si heterojunction diodes for solar cell applications

Weijie Du, Masakazu Baba, Kaoru Toko, Kosuke O. Hara, Kentaro Watanabe, Takashi Sekiguchi, Noritaka Usami, and Takashi Suemasu

Citation: *Journal of Applied Physics* **115**, 223701 (2014); doi: 10.1063/1.4882117

View online: <http://dx.doi.org/10.1063/1.4882117>

View Table of Contents: <http://scitation.aip.org/content/aip/journal/jap/115/22?ver=pdfcov>

Published by the [AIP Publishing](#)

---

### Articles you may be interested in

Transport mechanisms and effective Schottky barrier height of ZnO/a-Si:H and ZnO/c-Si:H heterojunction solar cells

*J. Appl. Phys.* **114**, 184505 (2013); 10.1063/1.4831661

Electrical transport properties of isolated carbon nanotube/Si heterojunction Schottky diodes

*Appl. Phys. Lett.* **103**, 193111 (2013); 10.1063/1.4829155

On the electrical behavior of V<sub>2</sub>O<sub>5</sub>/4H-SiC Schottky diodes

*J. Appl. Phys.* **113**, 224503 (2013); 10.1063/1.4809543

Modified, semiconducting graphene in contact with a metal: Characterization of the Schottky diode

*Appl. Phys. Lett.* **97**, 163101 (2010); 10.1063/1.3495777

Graphite based Schottky diodes formed on Si, GaAs, and 4H-SiC substrates

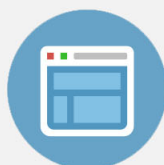
*Appl. Phys. Lett.* **95**, 222103 (2009); 10.1063/1.3268788

---

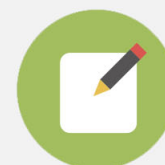


## Re-register for Table of Content Alerts

Create a profile.



Sign up today!



# Analysis of the electrical properties of Cr/n-BaSi<sub>2</sub> Schottky junction and n-BaSi<sub>2</sub>/p-Si heterojunction diodes for solar cell applications

Weijie Du,<sup>1</sup> Masakazu Baba,<sup>1</sup> Kaoru Toko,<sup>1</sup> Kosuke O. Hara,<sup>2</sup> Kentaro Watanabe,<sup>1,3</sup> Takashi Sekiguchi,<sup>3</sup> Noritaka Usami,<sup>2,4</sup> and Takashi Suemasu<sup>1,4</sup>

<sup>1</sup>*Institute of Applied Physics, University of Tsukuba, Tsukuba, Ibaraki 305-8573, Japan*

<sup>2</sup>*Graduate School of Engineering, Nagoya University, Chikusa-ku, Nagoya 464-8603, Japan*

<sup>3</sup>*National Institute for Materials Science, Tsukuba, Ibaraki 305-0044, Japan*

<sup>4</sup>*Core Research for Evolutional Science and Technology, Japan Science and Technology Agency, Chiyoda, Tokyo 102-0075, Japan*

(Received 13 May 2014; accepted 27 May 2014; published online 9 June 2014)

Current status and future prospects towards BaSi<sub>2</sub> pn junction solar cells are presented. As a preliminary step toward the formation of BaSi<sub>2</sub> homojunction diodes, diodes with a Cr/n-BaSi<sub>2</sub> Schottky junction and an n-BaSi<sub>2</sub>/p-Si hetero-junction have been fabricated to investigate the electrical properties of the n-BaSi<sub>2</sub>. Clear rectifying properties were observed in the current density versus voltage characteristics in both diodes. From the capacitance-voltage measurements, the built-in potential,  $V_D$ , was 0.53 V in the Cr/n-BaSi<sub>2</sub> Schottky junction diode, and the Schottky barrier height was 0.73 eV calculated from the thermoionic emission theory; the  $V_D$  was about 1.5 V in the n-BaSi<sub>2</sub>/p-Si hetero-junction diode, which was consistent with the difference in the Fermi level between the n-BaSi<sub>2</sub> and the p-Si. © 2014 AIP Publishing LLC. [<http://dx.doi.org/10.1063/1.4882117>]

## I. INTRODUCTION

In recent years, thin-film solar cells such as Cu(In,Ga)Se<sub>2</sub>, Cu<sub>2</sub>ZnSnS<sub>4</sub>, and CdTe have been attracting so much attention due to their high efficiency and low cost.<sup>1–5</sup> We think that barium disilicide (BaSi<sub>2</sub>) could be another candidate material.<sup>6,7</sup> The band gap of BaSi<sub>2</sub> is approximately 1.3 eV that matches the solar spectrum better than crystalline Si.<sup>8,9</sup> Both theoretical and experimental researches revealed that BaSi<sub>2</sub> has a very large absorption coefficient of over  $3 \times 10^4 \text{ cm}^{-1}$  for photon energies greater than 1.5 eV.<sup>10,11</sup> We have already grown high-quality BaSi<sub>2</sub> epitaxial layers on both Si(111) and Si(001) substrates even though BaSi<sub>2</sub> has an orthorhombic crystal structure.<sup>12–15</sup> We have further formed polycrystalline BaSi<sub>2</sub> layers on <111>-oriented Si films prepared on SiO<sub>2</sub> using an Al-induced crystallization method.<sup>16</sup> Besides, the undoped n-BaSi<sub>2</sub> has a large minority-carrier (holes) diffusion length ( $\sim 10 \mu\text{m}$ ) and thereby a long minority carrier lifetime ( $> 10 \mu\text{s}$ ).<sup>17–19</sup> These results have suggested that BaSi<sub>2</sub> is a very promising material for thin-film solar cell applications. To form BaSi<sub>2</sub> homojunction diodes, the properties of BaSi<sub>2</sub> thin-films doped with impurities such as Cu, Ag, Sb, P, As, In, Al, and B have also been investigated.<sup>20–26</sup> Among these elements, Sb and B were proved to be the suitable candidates for n<sup>+</sup>-BaSi<sub>2</sub> and p<sup>+</sup>-BaSi<sub>2</sub>, respectively. Their diffusion coefficients are another important parameter that should be taken into account. Most impurities, such as Al, Sb, and As, except B have large diffusion coefficients in BaSi<sub>2</sub> layers.<sup>27–29</sup>

As a next step toward forming a BaSi<sub>2</sub> homojunction diode on a Si substrate, we need to investigate the electrical properties of an undoped n-type BaSi<sub>2</sub> film, which is to be an active layer in a solar cell. Due to the small electron affinity of BaSi<sub>2</sub> (3.2 eV), band offsets exist at the BaSi<sub>2</sub>/Si interface,<sup>30,31</sup> that is, 0.8 eV for the conduction band, and 0.6 eV for the valence band. These values are predicted from the

electron affinities of BaSi<sub>2</sub> and Si. The band offsets block the photocurrent flowing across the BaSi<sub>2</sub>/Si interface. An Sb-doped n<sup>+</sup>-BaSi<sub>2</sub>/p<sup>+</sup>-Si tunnel junction (TJ) solved this problem.<sup>32–34</sup> Recently, we have achieved large photocurrent corresponding to the internal quantum efficiency exceeding 70% for the 400 nm-thick undoped n-BaSi<sub>2</sub> layer grown on the Sb-doped n<sup>+</sup>-BaSi<sub>2</sub>/p<sup>+</sup>-Si TJ.<sup>35</sup> The remaining process is the formation of p-BaSi<sub>2</sub> layer on the undoped n-BaSi<sub>2</sub> layer to complete the BaSi<sub>2</sub> homojunction diode. However, there has been no report even on the built-in potential,  $V_D$ , in a BaSi<sub>2</sub>/Si heterojunction diode or in a metal/BaSi<sub>2</sub> Schottky junction diode, which is one of the most fundamental electrical properties in semiconductors. In an n-BaSi<sub>2</sub>/p-Si heterojunction diode, for example, the  $V_D$  is given ideally by the difference in work function between the n-BaSi<sub>2</sub> and p-Si. Assuming that the effective density of states of conduction band,  $N_C$ , is approximately  $2.6 \times 10^{19} \text{ cm}^{-3}$  from the effective mass tensors of electron in BaSi<sub>2</sub>,<sup>11</sup> the separation of the bottom of the conduction band,  $E_C$ , from the Fermi level,  $E_F$ , that is  $E_C - E_F$ , can be estimated using the value of electron concentration. Thus, the work function of the n-BaSi<sub>2</sub> can be calculated. The same is true for the p-Si. In this article, we grew an undoped n-BaSi<sub>2</sub> layer on a p-Si(111) for that purpose. An undoped n-BaSi<sub>2</sub> layer was also formed on the TJ, and a Schottky junction was formed on top of the n-BaSi<sub>2</sub> with Cr for comparison. Then, we measured the current-density versus voltage ( $J$ - $V$ ) and capacitance-voltage ( $C$ - $V$ ) characteristics of the above two diodes and compare their  $V_D$ 's with those predicted from their work functions.

## II. EXPERIMENTAL

An ion-pumped molecular beam epitaxy (MBE) system was used for the growth of samples. For the Schottky junction diode, the p<sup>+</sup>-Si ( $\rho \leq 0.01 \Omega\text{-cm}$ ) substrate was adopted.

First, the substrate was heated at 900 °C for 30 min for cleaning the surface. A thin (~5 nm) BaSi<sub>2</sub> template layer was then grown by Ba deposition on the Si substrate at 500 °C for 5 min (reactive deposition epitaxy; RDE). The template was used to control the crystal orientation of the BaSi<sub>2</sub> overlayers. An approximately 30-nm-thick Sb-doped n<sup>+</sup>-BaSi<sub>2</sub> layer was grown at 550 °C by MBE for 20 min, to form a TJ with the p<sup>+</sup>-Si substrate. After that, a 1150-nm-thick undoped n-BaSi<sub>2</sub> layer was grown by MBE for 15 h at 600 °C. After the growth, 1-mm-diameter front-surface Au/Cr electrodes were formed by vacuum evaporation and the back-surface Al electrodes by sputtering. For the heterojunction diode, the p-Si substrate ( $\rho = 0.1 \Omega\cdot\text{cm}$ ) was used. First, a thin BaSi<sub>2</sub> template layer was grown by RDE at 500 °C. After that, an approximately 650-nm-thick undoped n-BaSi<sub>2</sub> layer was grown by MBE at 600 °C for 590 min. In order to facilitate to make ohmic contacts on the front-surface, another 10-nm-thick Sb-doped n<sup>+</sup>-BaSi<sub>2</sub> layer was grown. To avoid the Sb diffusion into the undoped n-BaSi<sub>2</sub> layer, the growth temperature was decreased to 500 °C for the n<sup>+</sup>-BaSi<sub>2</sub> layer. Finally, 0.5-mm-diameter front-surface Al electrodes were formed by sputtering. Backside electrodes were also formed with Al by sputtering. The electrical properties were measured at room temperature (RT).

### III. RESULTS AND DISCUSSION

#### A. Cr/n-BaSi<sub>2</sub> Schottky junction diode

Figure 1 shows the  $J$ - $V$  characteristics of the sample measured at RT. The current increased rapidly as the positive bias was applied to the Au/Cr electrode with respect to the p-Si substrate. Clear rectifying properties were observed in this sample, indicating that the Schottky junction was surely formed on the surface of the thick undoped BaSi<sub>2</sub> layers grown on the TJ. The series resistance,  $R_s$ , can be deduced from the slope of the  $I(dV/dI)$  versus  $I$  plot in a large  $I$  region, and the shunt resistance,  $R_{sh}$ , from the slope of  $dV/dI$  at around  $V = 0$ .<sup>36,37</sup> They were 180  $\Omega$  and 1 M $\Omega$ , respectively. The logarithmic plot of  $J$  with respect to  $V$  is inserted in Fig. 1, in which the series resistance and shunt resistance were

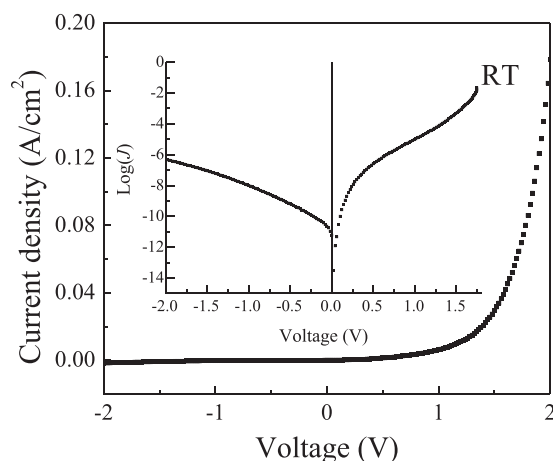


FIG. 1.  $J$ - $V$  characteristics of the Schottky junction diode measured at RT. The logarithmic plot is inserted. The bias voltage is applied to the Au/Cr electrode with respect to the p-Si substrate.

subtracted. The reverse saturation current density  $J_S$  can be deduced from the intercept of the straight line of the  $\text{Log}(J)$ - $V$  plot at  $V=0$  and was found to be  $6.1 \times 10^{-6} \text{ A/cm}^2$ . For a Schottky junction diode, the reverse saturation current density  $J_S$  can be expressed by the thermoionic emission theory:<sup>38</sup>

$$J_S = A^* T^2 \exp\left(-\frac{q\phi_S}{k_B T}\right), \quad (1)$$

where  $A^*$  is the effective Richardson constant,  $k_B$  the Boltzmann constant,  $q\phi_S$  the barrier height for electrons in the metal. The  $q\phi_S$  was calculated to be 0.73 eV for this Schottky junction. This value is smaller than that predicted from the electron affinity of BaSi<sub>2</sub> (3.2 eV) and the work function of Cr (4.5 eV). Thus, a thin interfacial layer is likely to exist between the Cr and the n-BaSi<sub>2</sub> due to the oxidation of the BaSi<sub>2</sub> surface, and voltages also drop at the interfacial layer.<sup>39,40</sup>

Figure 2(a) shows the  $1/C^2$  versus  $V$  plot of the Schottky junction diode. The  $V_D$  can be deduced by extending the straight line to the voltage axis and it was found to be 0.53 V. The positive ionized donor density,  $N_D^+$ , near the surface region of the n-BaSi<sub>2</sub> layer, was calculated to be  $3 \times 10^{16} \text{ cm}^{-3}$  from the  $C$ - $V$  characteristics, assuming that the permittivity of BaSi<sub>2</sub> approaches 15 for long wavelengths.<sup>11,41</sup> Figure 2(b) shows a simple band diagram of the Cr/n-BaSi<sub>2</sub> Schottky junction according to the Schottky-Mott model.<sup>42</sup>

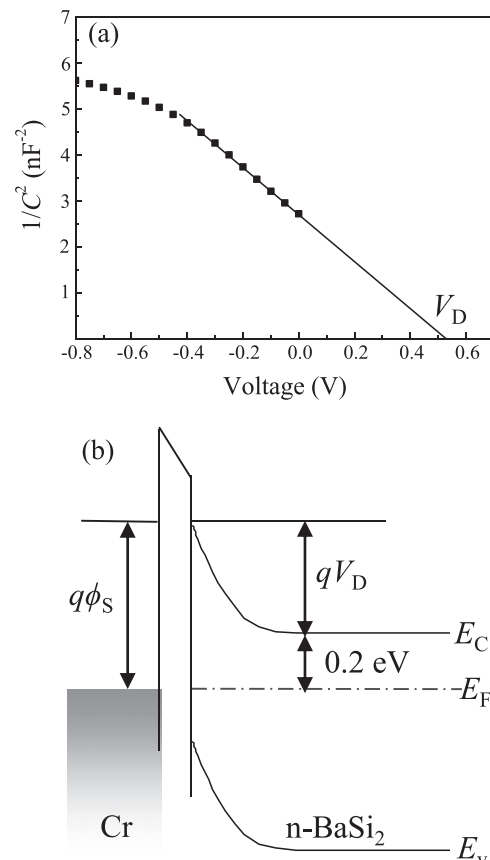


FIG. 2. (a)  $1/C^2$  versus  $V$  plot of the Schottky junction diode and a line for fitting. (b) Band diagram of the Cr/n-BaSi<sub>2</sub> Schottky junction.

The  $E_C - E_F$  was determined to be 0.2 eV in the n-BaSi<sub>2</sub> assuming that it is equal to  $q(\phi_S - V_D)$ . The electron concentration,  $n$ , is given by

$$n = N_C \exp\left(-\frac{E_C - E_F}{k_B T}\right). \quad (2)$$

Assuming complete ionization of impurity atoms in the n-BaSi<sub>2</sub>, and thereby  $n = N_D^+ = 3 \times 10^{16} \text{ cm}^{-3}$ , the  $E_C - E_F$  was thus calculated to be 0.18 eV at RT. This value is consistent with  $q(\phi_S - V_D)$ , thereby the band diagram shown in Fig. 2(b).

### B. n-BaSi<sub>2</sub>/p-Si hetero-junction diode

Now let us discuss the electric properties of the n-BaSi<sub>2</sub>/p-Si heterojunction diode. Figure 3(a) shows the  $J$ - $V$  characteristics of the diode measured at RT. The bias voltage was applied to the p-Si substrate with respect to the n<sup>+</sup>-BaSi<sub>2</sub> top layer. Clear rectifying properties were also confirmed in this heterojunction diode. The  $R_s$  and  $R_{sh}$  were calculated to be 0.8 kΩ and 40 kΩ, respectively. The inserted figure shows the logarithmic plot of  $J$ - $V$  characteristics, where the  $R_s$  and  $R_{sh}$  were subtracted. The ideal factor of the diode, which should be between 1 and 2, was 1.7 under the bias voltages smaller than 0.3 V. However, this value increased to 14.6 when the bias voltage was higher than 0.5 V. This might be due to the carrier trapping at the defect

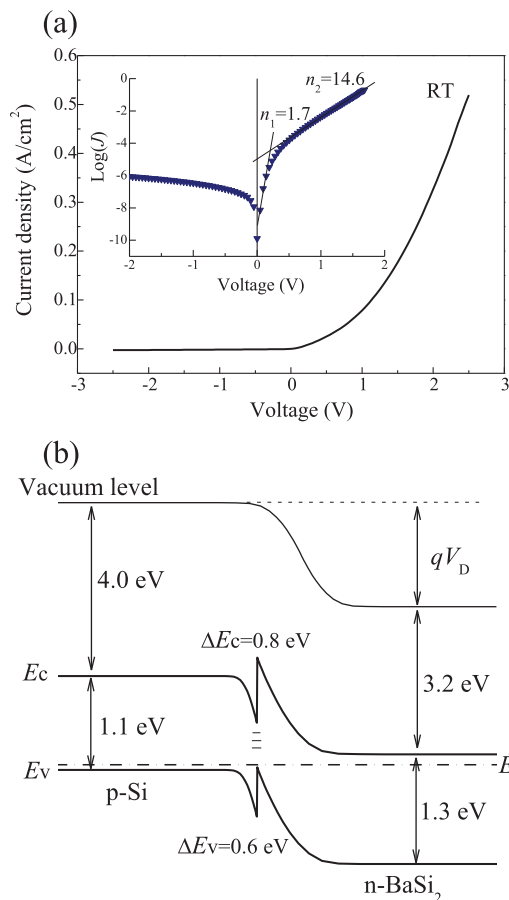


FIG. 3. (a)  $J$ - $V$  characteristics of the hetero-junction diode measured at RT. The insertion is the logarithmic plot of  $J$ - $V$  characteristics. (b) Band diagram of n-BaSi<sub>2</sub>/p-Si hetero-junction.

states at the interface and a nonlinear series resistance in the diode structure. The reverse saturation current density  $J_0$  was deduced to be  $1.2 \times 10^{-4} \text{ A/cm}^2$  from the  $\text{Log}(J)$  versus  $V$  plot in the inserted figure.

Figure 4(a) shows the  $1/C^2$  versus  $V$  plot of the sample. In our previous works, the electron density in the undoped n-BaSi<sub>2</sub> was usually of the order of  $10^{16} \text{ cm}^{-3}$  from the Hall measurement.<sup>43</sup> This value is smaller by one order of magnitude than that in the p-Si substrate ( $p \sim 2 \times 10^{17} \text{ cm}^{-3}$ ) used in this work. Thus, it is reasonable to think that the depletion region extended mostly toward the n-BaSi<sub>2</sub> layer. Figure 4(b) shows the  $n$  distribution in the n-BaSi<sub>2</sub> layer assuming complete ionization of impurity atoms. The average electron density was about  $2 \times 10^{16} \text{ cm}^{-3}$ . Homogeneous carrier concentration profile indicated the high quality of the BaSi<sub>2</sub> epitaxial thin film. As a result, the  $1/C^2$  versus  $V$  plot was well fitted by a linear broken line as shown in Fig. 4(a). The  $V_D$  was deduced to be about 1.5 V in this heterojunction diode. The  $E_C - E_F$  is calculated to be 0.19 eV for  $n = 2 \times 10^{16} \text{ cm}^{-3}$  in BaSi<sub>2</sub>, while the separation of  $E_F$  from the top of the valence band,  $E_V$ , that is  $E_F - E_V$ , is estimated to be 0.10 eV using  $p = 2 \times 10^{17} \text{ cm}^{-3}$  in the p-Si substrate. Thereby, the difference in work function between the n-BaSi<sub>2</sub> and p-Si is approximately  $4.0 + (1.1 - 0.1) - (3.2 + 0.19) \cong 1.6 \text{ eV}$ . This value is consistent with the experimentally obtained  $V_D$  of 1.5 V, as shown in Fig. 4(a).

On the basis of these results on the two kinds of diodes, we conclude that the band diagrams of the undoped n-BaSi<sub>2</sub>/p-Si and the metal/BaSi<sub>2</sub> heterojunctions are well explained by a conventional way widely used in semiconductor physics although BaSi<sub>2</sub> is really an unfamiliar

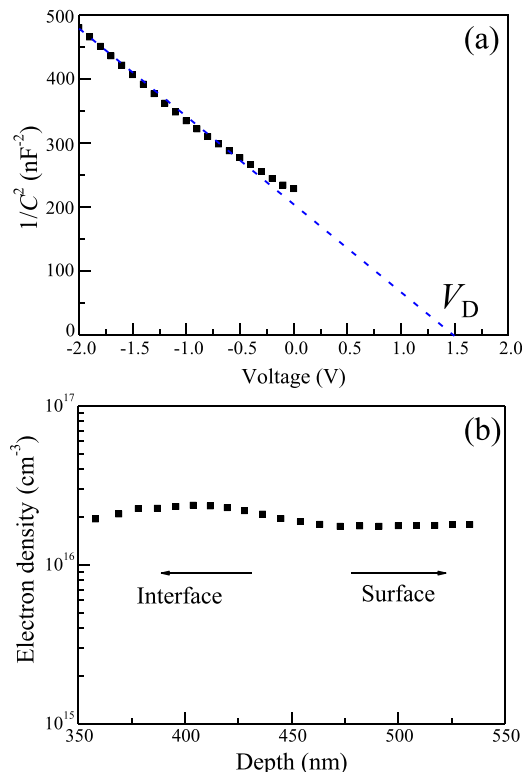


FIG. 4. (a)  $1/C^2$  versus  $V$  plot and a broken line for fitting (blue). The bias voltage is applied to the p-Si substrate with respect to the n<sup>+</sup>-BaSi<sub>2</sub>. (b) Electron density distribution in the BaSi<sub>2</sub> layer.

semiconductor material. These results facilitate us to design the device structure of BaSi<sub>2</sub> homojunction and heterojunctions solar cells.

#### IV. CONCLUSIONS

We have formed the Cr/n-BaSi<sub>2</sub> Schottky junction and n-BaSi<sub>2</sub>/p-Si heterojunction diodes. In both samples, clear rectifying properties were observed in the  $J$ - $V$  characteristics at RT. In the Schottky junction diode, the  $J_S$  was  $6.1 \times 10^{-6}$  A/cm<sup>2</sup>, the Schottky barrier height was calculated to be 0.73 eV and the  $V_D$  deduced from the  $1/C^2$  versus  $V$  plot, was found to be 0.53 V. These results were in good agreement with the Schottky-Mott model. In the heterojunction diode, the  $V_D$  was found to be 1.5 V, which was well explained by the difference in  $E_F$  between the n-BaSi<sub>2</sub> and p-Si. The reverse saturation current density was  $1.2 \times 10^{-4}$  A/cm<sup>2</sup>. The electron concentrations of the undoped n-BaSi<sub>2</sub> layers were of the order of  $10^{16}$  cm<sup>-3</sup> in both samples from the  $C$ - $V$  measurement.

#### ACKNOWLEDGMENTS

This work was financially supported by Core Research for Evolutional Science and Technology, Japan Science and Technology Agency (JST-CREST).

- <sup>1</sup>M. A. Green, *Prog. Photovolt. Res. Appl.* **20**, 472 (2012).
- <sup>2</sup>S. Ahmed, K. B. Reuter, O. Gunawan, L. Guo, L. T. Romankiw, and H. Deligianni, *Adv. Eng. Mater.* **2**, 253 (2012).
- <sup>3</sup>B. M. Basol, *J. Appl. Phys.* **55**, 601 (1984).
- <sup>4</sup>M. A. Green and S. R. Wenham, *Appl. Phys. Lett.* **65**, 2907 (1994).
- <sup>5</sup>W. Jaegermann, A. Klein, and T. Mayer, *Adv. Mater.* **21**, 4196 (2009).
- <sup>6</sup>J. Evers, G. Oehlinger, and A. Weiss, *Angew. Chem. Int. Ed.* **16**, 659 (1977).
- <sup>7</sup>M. Imai and T. Hirano, *J. Alloys Compd.* **224**, 111 (1995).
- <sup>8</sup>T. Nakamura, T. Suemasu, K. Takakura, F. Hasegawa, A. Wakahara, and M. Imai, *Appl. Phys. Lett.* **81**, 1032 (2002).
- <sup>9</sup>T. Suemasu, K. Morita, and M. Kobayashi, *J. Cryst. Growth* **301–302**, 680 (2007).
- <sup>10</sup>K. Toh, T. Saito, and T. Suemasu, *Jpn. J. Appl. Phys., Part 1* **50**, 068001 (2011).
- <sup>11</sup>D. B. Migas, V. L. Shaposhnikov, and V. E. Borisenko, *Phys. Status Solidi B* **244**, 2611 (2007).
- <sup>12</sup>Y. Inomata, T. Nakamura, T. Suemasu, and F. Hasegawa, *Jpn. J. Appl. Phys., Part 1* **43**, 4155 (2004).
- <sup>13</sup>Y. Inomata, T. Suemasu, T. Izawa, and F. Hasegawa, *Jpn. J. Appl. Phys., Part 2* **43**, L771 (2004).
- <sup>14</sup>K. Toh, K. O. Hara, N. Usami, N. Saito, N. Yoshizawa, K. Toko, and T. Suemasu, *Jpn. J. Appl. Phys., Part 1* **51**, 095501 (2012).
- <sup>15</sup>R. Takabe, K. Nakamura, M. Baba, W. Du, M. Ajmal Khan, K. Toko, M. Sasase, K. O. Hara, N. Usami, and T. Suemasu, *Jpn. J. Appl. Phys., Part 1* **53**, 04ER04 (2014).
- <sup>16</sup>D. Tsukada, Y. Matsumoto, R. Sasaki, M. Takeichi, T. Saito, N. Usami, and T. Suemasu, *Appl. Phys. Express* **2**, 051601 (2009).
- <sup>17</sup>M. Baba, K. Toh, K. Toko, N. Saito, N. Yoshizawa, K. Jiptner, T. Sekiguchi, K. O. Hara, N. Usami and T. Suemasu, *J. Cryst. Growth* **348**, 75 (2012).
- <sup>18</sup>K. O. Hara, N. Usami, K. Nakamura, R. Takabe, M. Baba, K. Toko, and T. Suemasu, *Appl. Phys. Express* **6**, 112302 (2013).
- <sup>19</sup>R. Takabe, K. O. Hara, M. Baba, W. Du, N. Shimada, K. Toko, N. Usami, and T. Suemasu, *J. Appl. Phys.* **115**, 193510 (2014).
- <sup>20</sup>M. Kobayashi, Y. Matsumoto, Y. Ichikawa, D. Tsukada, and T. Suemasu, *Appl. Phys. Express* **1**, 051403 (2008).
- <sup>21</sup>M. Ajmal Khan, T. Saito, K. Nakamura, M. Baba, W. Du, K. Toh, K. Toko, and T. Suemasu, *Thin Solid Films* **522**, 95 (2012).
- <sup>22</sup>M. Ajmal Khan, K. O. Hara, W. Du, M. Baba, K. Nakamura, M. Suzuno, K. Toko, N. Usami, and T. Suemasu, *Appl. Phys. Lett.* **102**, 112107 (2013).
- <sup>23</sup>R. Takabe, M. Baba, K. Nakamura, W. Du, M. A. Khan, S. Koike, K. Toko, K. O. Hara, N. Usami, and T. Suemasu, *Phys. Status Solidi C* **10**, 1753 (2013).
- <sup>24</sup>K. O. Hara, Y. Hoshi, N. Usami, Y. Shiraki, K. Nakamura, K. Toko, and T. Suemasu, *Thin Solid Films* **557**, 90 (2014).
- <sup>25</sup>K. O. Hara, Y. Hoshi, N. Usami, Y. Shiraki, K. Nakamura, K. Toko, and T. Suemasu, *Thin Solid Films* **534**, 470 (2013).
- <sup>26</sup>K. O. Hara, N. Usami, Y. Hoshi, Y. Shiraki, M. Suzuno, K. Toko, and T. Suemasu, *Jpn. J. Appl. Phys., Part 1* **50**, 121202 (2011).
- <sup>27</sup>K. Nakamura, M. Baba, M. Ajmal Khan, W. Du, M. Sasase, K. O. Hara, N. Usami, K. Toko, and T. Suemasu, *J. Appl. Phys.* **113**, 053511 (2013).
- <sup>28</sup>K. Nakamura, K. Toh, M. Baba, K. M. Ajmal, W. Du, K. Toko, and T. Suemasu, *J. Cryst. Growth* **378**, 189 (2013).
- <sup>29</sup>N. Zhang, K. Nakamura, M. Baba, K. Toko, and T. Suemasu, *Jpn. J. Appl. Phys., Part 1* **53**, 04ER02 (2014).
- <sup>30</sup>T. Suemasu, K. Morita, M. Kobayashi, M. Saida, and M. Sasaki, *Jpn. J. Appl. Phys., Part 2* **45**, L519 (2006).
- <sup>31</sup>B. E. Umirzakov, D. A. Tashmukhamedova, E. U. Boltaev and A. A. Dzhrakhalov, *Mater. Sci. Eng. B* **101**, 124 (2003).
- <sup>32</sup>W. Du, T. Saito, M. Ajmal Khan, K. Toko, N. Usami, and T. Suemasu, *Jpn. J. Appl. Phys., Part 1* **51**, 04DP01 (2012).
- <sup>33</sup>T. Saito, Y. Matsumoto, M. Suzuno, M. Takeishi, R. Sasaki, N. Usami, and T. Suemasu, *Appl. Phys. Express* **3**, 021301 (2010).
- <sup>34</sup>T. Suemasu, T. Saito, K. Toh, A. Okada, and M. Ajmal Khan, *Thin Solid Films* **519**, 8501 (2011).
- <sup>35</sup>W. Du, M. Suzuno, M. Ajma Khan, K. Toh, M. Baba, K. Nakamura, K. Toko, N. Usami, and T. Suemasu, *Appl. Phys. Lett.* **100**, 152114 (2012).
- <sup>36</sup>H. Norde, *J. Appl. Phys.* **50**, 5052 (1979).
- <sup>37</sup>S. K. Cheung and N. W. Cheung, *Appl. Phys. Lett.* **49**, 85 (1986).
- <sup>38</sup>F. A. Padovani and R. Stratton, *Solid-State Electron.* **9**, 695 (1966).
- <sup>39</sup>S. M. Sze, *Physics of Semiconductor Devices*, 3rd ed. (Wiley, New York, 1981), p. 140.
- <sup>40</sup>A. M. Cowley and S. M. Sze, *J. Appl. Phys.* **36**, 3212 (1965).
- <sup>41</sup>N. A. A. Latiff, T. Yoneyama, T. Shibutami, K. Matsumaru, K. Toko, and T. Suemasu, *Phys. Status Solidi C* **10**, 1759 (2013).
- <sup>42</sup>N. F. Mott, *Proc. Camb. Philos. Soc.* **34**, 568 (1938).
- <sup>43</sup>K. Morita, Y. Inomata, and T. Suemasu, *Thin Solid Films* **508**, 363 (2006).